



Published in final edited form as:

J Orthop Res. 2020 January ; 38(1): 117–127. doi:10.1002/jor.24406.

Stem Cell-Derived Extracellular Vesicles Attenuate the Early Inflammatory Response after Tendon Injury and Repair

Hua Shen¹, Susumu Yoneda¹, Yousef Abu-Amer^{1,2}, Farshid Guilak^{1,2}, Richard H. Gelberman¹

¹Department of Orthopaedic Surgery, Washington University School of Medicine, St. Louis, MO, USA

²Shriners Hospitals for Children – St. Louis, St. Louis, MO, USA

Abstract

Adipose-derived stem cells (ASCs) have the potential to enhance tendon repair via paracrine regulation of the inflammatory response to injury. Extracellular vesicles (EVs), which are secreted by ASCs, have shown promise in mediating this process. This study was designed to evaluate the effect of ASC EVs on early tendon healing using a mouse Achilles tendon injury and repair model. EVs were isolated from the conditioned medium of naïve and interferon gamma-primed ASCs and applied to the repair site via a collagen sheet. Tendon healing was assessed in NF- κ B-luciferase reporter mice up to 7 days after suture repair. As anticipated, repair site NF- κ B activity increased greater than 2-fold following tendon repair. Treatment with EVs from primed but not naïve ASCs effectively suppressed the response. Accordingly, the pro-inflammatory genes *Il1b* and *Ifng* were both dramatically increased in repaired tendons, while primed, but not naïve ASC EVs attenuated the response. Compared with control repairs, primed ASC EVs further reduced the rate of post-repair tendon gap formation and rupture and facilitated collagen formation at the injury site. Additional experiments demonstrated that EVs target macrophages and that primed ASC EVs were most effective in blocking macrophage NF- κ B activity. Collectively, the findings of this study demonstrate that primed ASC EVs, similar to ASCs, attenuate the early tendon inflammatory response after injury via modulation of the macrophage inflammatory response. Clinical significance: These findings introduce a new cell-free therapy, derived from stem cells, for tendon repair with the potential for improved therapeutic efficacy and safety.

Keywords

Extracellular vesicle; mesenchymal stem cell; exosome; tendon injury; inflammation

Correspondence: Hua Shen, Ph.D., Department of Orthopaedic Surgery, Washington University School of Medicine, 660 South Euclid Avenue, St. Louis, MO 63110, USA. Telephone: 314-747-5707; fax number: 314-362-0334; hshen22@wustl.edu.

Author Contributions Statement: HS, conceived and designed the study, developed research models, collected, analyzed, and interpreted data, and drafted the manuscript; SY, contributed to the development of animal model and data collection; FG, contributed to study design and data interpretation and edited the manuscript; YA-A, contributed to study design and method development and edited the manuscript; RHG, contributed to the development of animal model, data interpretation, and manuscript preparation. All authors read and approved the final version of the manuscript.

INTRODUCTION

Tendon and ligament injuries comprise 45% of musculoskeletal trauma in the United States.^{1,2} Tendon transections are debilitating as intense post-repair inflammatory responses coupled with inadequate regenerative processes impair tendon gliding and reduce repair site strength.³⁻⁵ Frequently encountered complications following tendon suture are the formation of adhesions and the development of repair site gap formation or rupture.^{3,6,7}

Recently, a number of clinically relevant mesenchymal stem cell (MSC)-based therapies with the potential to improve the outcomes of tendon repair have emerged.^{3,7-12} MSCs are regulatory signaling cells capable of paracrine regulation of cells' response to injury.¹³⁻¹⁶ Adipose-derived stem cells (ASCs), which represent a similar type of adult stem cell, have been found to shift the phenotypic response of infiltrating macrophages from a default pro-inflammatory M1 phenotype to an anti-inflammatory and pro-regenerative M2 phenotype, thereby facilitating tendon healing.^{10,11,17} While the underlying mechanisms remain elusive, extracellular vesicles (EVs) have been identified as one of primary paracrine effectors of ASCs.¹⁸⁻²¹ EVs are cell-derived vesicles that mediate cell-cell communication by delivering various functional molecules (e.g., proteins, mRNAs, and microRNAs) to selective recipient cells.²²⁻²⁵ Although nearly all cells can produce EVs, the composition and function of EVs are cell-type specific. MSC EVs from several origins including adipose tissue have recently been reported to modulate the macrophage inflammatory response^{21,24,26,27} and the function of MSC EVs may be further enhanced by priming MSCs with such inflammatory cytokine as interferon γ (IFN γ).^{21,26} Therefore, EVs produced by ASCs may provide an alternative to ASCs as a new potent therapeutic agent for tendon injury.

ASC EVs possess many attractive properties as a potential therapeutic candidate for tendon-specific application. Compared with other tissues, such as bone marrow, adipose tissue is abundant in the adult and contains a relatively high percentage of colony-forming unit cells.²⁸ While ASCs have shown great therapeutic potential for tendon repair,^{10,11,29} safety concerns have hindered their clinical application (i.e., tumorigenicity and undesired spontaneous differentiation).³⁰ As a cell-free agent, ASC EVs avoid the safety concerns. Notably, EVs possess a unique membrane structure, which can protect, carry, and deliver a variety of enriched functional molecules capable of modulating recipient cell functions.²²⁻²⁵ In this regard, EVs may also provide superior drug stability, target specificity, and delivery capacity/efficacy compared to soluble factors. Moreover, an improved understanding of the molecular basis of EV functions will allow further engineering of defined components within EVs to provide improved therapeutic efficacy and safety.

The goal of this study was to investigate the role of ASC-derived EVs in regulating tissue responses in the earliest phases of tendon healing in a clinically relevant mouse Achilles tendon injury and repair model. Our hypothesis was that EVs, as a primary effector of ASCs, will effectively attenuate the early tendon inflammatory response after injury and thereby facilitate tendon healing.

METHODS

Animals

All animal studies were conducted in accordance with the Public Health Service Policy on Humane Care and Use of Laboratory Animals and approved and overseen by the Washington University Institutional Animal Care and Use Committee. NF- κ B-GFP-luciferase (NGL) transgenic reporter mice for nuclear factor kappa-light-chain-enhancer of activated B cells (NF- κ B) and wild type FVB mice were purchased from The Jackson Laboratory (Bar Harbor, ME).³¹ Scleraxis-GFP (ScxGFP) tendon reporter mice were provided by Dr. Ronen Schweitzer.³² Mice were given ad libitum access to food and water and housed communally at a room temperature of 20–23°C on a 12-hour light/dark cycle.

Cell culture and EV preparation

Mouse macrophages were derived from bone marrow of femurs and tibiae of adult NGL or FVB mice of both sexes and cultured in a macrophage culture medium containing 10% L929 cell conditioned medium (a source of macrophage colony stimulating factor), 100 unit/ml penicillin, 100 μ g/ml streptomycin (Life Technologies, Grand Island, NY), and 10% fetal bovine serum (FBS; Life Technologies, catalog # 26140–079) in Minimum Essential Medium, Alpha (α -MEM; Corning, Manassas, VA, catalog # 10–022-CV). After five days, adherent cells were harvested and used for subsequent studies.

Mouse ASCs were isolated from the stromal vascular fraction of subcutaneous fat of adult ScxGFP or NGL mice of both sexes and expanded in ASC Culture Medium containing 10% FBS, 100 unit/ml penicillin, and 100 μ g/ml streptomycin in α -MEM as detailed elsewhere.²⁸

EVs were isolated from the conditioned medium of ASC culture. ASCs at passage 2 to 4 were primed with 100 ng/ml IFN γ (R&D Systems, Minneapolis, MN) overnight. The medium was subsequently removed. After three washes with sterile Dulbecco's Phosphate Buffered Saline (DPBS; Life Technologies), the cells were further cultured in an EV collection medium (2% EV-free FBS in α -MEM) for 48 hours. Conditioned medium from ASC culture (150 ml from approximately $2.5E+07$ cells per isolation) with or without IFN γ pre-treatment was collected and centrifuged at $500 \times g$ for 10 min and $10,000 \times g$ for 30 min at 4 °C to remove large vesicles. After passing through a 0.22 μ m filter, the medium was further centrifuged at $100,000 \times g$ for 90 min at 4°C. The resulting EV-free supernatant was collected as EV-free conditioned medium. The EV-containing precipitate was further washed and re-suspended in 70 μ l DPBS. Some isolated ASC EVs were fluorescently labeled with PKH26 (Sigma-Aldrich, St. Louis, MO). The EV-free FBS was prepared by ultracentrifugation of FBS at $100,000 \times g$ for 20 hours to remove EVs in the FBS.

Characterization of mouse ASCs and ASC-derived EVs

ASCs were assessed for their ability to form colony-forming units (CFUs) and by their surface marker expression with antibodies specific for MSC markers CD29 (BD Biosciences, clone 18/CD29), CD44 (eBiosciences, clone IM7), and CD90 (BD Biosciences, clone 5E10)³³ as previously described.²⁸

Isolated ASC EVs were negatively stained with 1% aqueous uranyl acetate (Ted Pella Inc., Redding, CA) and viewed on a JEOL 1200EX transmission electron microscope (JEOL USA, Peabody, MA). The size and concentration of EVs was determined at ZenBio Inc. (Research Triangle Park, NC) using qNano Gold (Izon Science Ltd. Christchurch, New Zealand). EV protein concentrations were determined with a Thermo Scientific™ Micro BCA™ Protein Assay Kit (Thermo Scientific, Rockford, IL). EV marker expression was determined by Western blot with either rabbit anti-CD9 (EXOAB-CD9A-1; System Biosciences) or rabbit anti-CD63 (EXOAB-CD63A-1, System Biosciences) antibodies followed by HRP-conjugated goat-anti-rabbit secondary antibodies (System Biosciences).

***In vitro* study design**

In vitro studies were conducted with EVs produced by IFN γ -primed and naïve mouse ASCs (iEVs and EVs). The impact of ASC EVs on the macrophage inflammatory response was evaluated in EV-macrophage co-culture. Macrophages were stimulated with the pro-inflammatory cytokine Interleukin 1 beta (IL-1 β). IL-1 β was chosen because it was the most significantly induced pro-inflammatory cytokine detected in the mouse Achilles tendon after injury and repair. To assess the EV-specific effect, EV collection medium (Medium) and EV-free conditioned medium from naïve and primed ASC culture (CM and iCM) were used as controls. The macrophage inflammatory responses were assessed via the NF- κ B-luciferase reporter expressed by the NGL mice for the NF- κ B-responsive luciferase activity and luciferase mRNA expression. All results were obtained from at least three independent experiments.

Macrophage assays

NGL macrophages (30,000 cells/cm²) were pre-treated with either one of the following: Medium, CM, iCM, EV or iEV for 24 hours (N=3–4 /condition in duplicate). EVs and iEVs were applied at a dose corresponding to an EV donor and recipient cell ratio of 20:1. The dose was determined based on a previously published study.¹⁷ The pre-treated cells were washed three times with DPBS. Macrophage NF- κ B activity was subsequently determined in cell lysates 6 hours after treatment with IL-1 β (5 ng/ml; R&D Systems, Minneapolis, MN) using a Dual-Luciferase Reporter Assay System (Promega, Madison, WI). The results were normalized by the protein concentrations of respective samples. Macrophage gene expression was assessed at 24 hours after IL-1 β (10 ng/ml) treatment in cell lysates by a SYBR green-based quantitative RT-PCR.²⁸

Achilles tendon injury and repair model

Achilles tendon 2/3 transection was conducted at the midpoint level between the calcaneal insertion and the musculotendinous junction of the right Achilles tendon. All transected tendons were repaired with a 2-strand modified Kessler technique with surface locking followed by a simple peripheral suture (8–0 Ethilon, Ethicon Inc; Fig. 2A).³⁴ Following repair, mice were allowed free movement after recovery from anesthesia.

***In vivo* delivery and detection of ASC EVs**

A thin collagen sheet was prepared as described previously.¹⁰ ASC EVs were loaded to the surface of the collagen sheet via their collagen binding properties.³⁵ The EV-laden collagen sheet was cut into strips (2.5 mm × 10 mm × 0.2 mm) that contained 5~6E+09 EVs from approximately one-half million ASCs and was applied around the repair site (Fig. 2A). The EV dose was determined based on the ASC dose used previously.¹⁰ The distribution of PKH26-labeled ASC EVs in Achilles tendons was determined in 6-month old ScxGFP tendon reporter mice (N=2) 7 days after implantation by fluorescence microscopy.

***In vivo* study design**

To assess the impact of ASC EVs on the early tendon healing response after injury, a total of 32 adult NGL mice of both sexes (3–4 months, weight 27±5 g) were used. After Achilles tendon partial transection and repair, the mice were randomly divided into three groups: (1) collagen sheet only (Repair, N=11), (2) collagen sheet loaded with EVs from naïve ASCs (+EV, N=11), and (3) collagen sheet loaded with EVs from IFN γ -primed ASCs (+iEV, N=10). NF- κ B activity at the repair site was determined in live mice via bioluminescence imaging at 1 day before (Pre) and 1, 3, and 7 days after (D1, D3, and D7) repair and treatment (N=4/group for Repair and +EV group, N=6 for +iEV group). All mice were euthanized 7 days after repair. Repaired tendons were surgically exposed as shown in the right panel of Fig. 2A. The integrity of repaired tendons was first assessed under a dissecting microscope. Postoperative gap formation and rupture were defined as partial and complete loss of the continuity of the repaired tendons, respectively. The assessed tendons were then dissected out for either gene expression (N=7/group) or histological assessment (N=4, 3, and 3 for Repair, +EV, and +iEV group, respectively).

NF- κ B-luciferase imaging *in vivo*

Mice were injected intraperitoneally with D-luciferin (150mg/kg in PBS; Gold Biotechnology, St. Louis, MO) and imaged 10 minutes after injection under isoflurane anesthesia (2% vaporized in O₂) in an IVIS 50 (PerkinElmer, Waltham, MA). Images were acquired with Living Image 4.3.1 software (Xenogen Corp., Alameda, CA). Injury site total photon flux (photons/sec) was measured from software-defined contour region of interest (ROI) that covers the injury site using Living Image 2.6 software. The result was normalized by the total photon flux of matching ROI of contralateral uninjured limb and expressed as a ratio of pre-injury level.

Total RNA isolation and quantitative RT-PCR

Total RNA from cultured cells were isolated with TRIzol Reagent (Life Technologies) and RNeasy Mini Spin Column (Qiagen Sciences, MD, USA) as previously described.²⁸ Achilles tendons were pulverized with a Mikro-Dismembrator U (Sartorius AG, Goettingen, Germany) and extracted in TRIzol Reagent (Life Technologies). Total RNAs were isolated via phase separation using a Phase Lock Gel (5 Prime GmbH, Hamburg, Germany) and purified with RNeasy MinElute[®] Spin Columns (Qiagen Sciences, Germantown, MD). 500 ng of isolated total RNAs were reversely transcribed into cDNAs using a SuperScript[™] IV VILO[™] Master Mix (Life Technologies). The relative abundances of genes of interest were

determined by SYBR green real-time PCR using Qiagen (Table 1) or custom primers (Table 2). *Ipo8* was used as an endogenous reference gene. Changes in tendon gene expression were determined by the comparative Ct method and shown as fold changes relative to the expression levels in contralateral intact tendons. For genes that were near the detection limit in intact tendons, the results were reported as relative mRNA abundance (2^{-Ct}).

Achilles tendon histology

Achilles tendons were fixed in 4% paraformaldehyde in PBS, embedded in paraffin, sectioned coronally at 5 μ m thickness, and stained with a pentachrome stain kit (American MasterTech, Lodi, CA) as described previously.²⁹ Collagen in stained sections exhibits a bright red-orange color. The percentage of collagen-stained area in a 1.2 mm tendon fragment that covers the site of tendon injury was determined with the area analysis tool of Adobe Photoshop CC 2015.5 (Adobe Systems Incorporated).

Statistical analysis

All data are shown as mean \pm standard deviation. One-way analysis of variance (ANOVA) followed by Tukey's or Dunn's post-hoc tests (when appropriate) were performed to compare gene expression levels, macrophage activities, or histomorphometry results among groups; two-tailed paired Student's t-tests were used to compare gene expression levels and EV size and yield between two groups; a two-way ANOVA followed by Student-Newman-Keuls (SNK) multiple comparisons were used to compare the effects of treatment and time on NF- κ B activity at the repair site. An "N-1" Chi-squared test was used to compare the post-operative complication rate between treated and control repair groups.³⁶ The significance level was set at $P < 0.05$.

RESULTS

Isolated ASC EVs exhibit the properties of exosome

Mouse ASCs exhibited a CFU frequency of approximately 1 in 300 and an average population doubling time of 1.68 ± 0.74 days ($N=5$ isolations), similar to those reported in the literature.²⁸ Immunostaining revealed that nearly all isolated cells expressed the MSC markers CD29, CD44, and CD90 (Fig. 1A). The ASCs with and without IFN γ priming yielded similar amounts of vesicles ($1.61E+09 \pm 1.81E+09$ and $1.67E+09 \pm 4.64E+08$ particles/ml culture, respectively; $N=3$ /group, $P=0.995$). The resulting iEVs and EVs were of similar size (mode diameter 108 ± 2 nm and 113 ± 3 nm) and were within the size range of exosomes.²² Transmission electron microscopy also showed that EVs and iEVs exhibited similar size and morphology (left and middle panels in Fig. 1B) and that the EV collection medium was free from EVs (right panel in Fig. 1B). Western blot further confirmed that ASC EVs expressed the exosome markers CD9 and CD63 (Fig. 1C), thus possessing the properties of exosome.

ASC EVs target infiltrating inflammatory cells at the site of tendon injury

Partial tendon transection and repair was generated at the right Achilles tendon of adult mice (Fig. 2A). Approximately $5 \sim 6E+09$ EVs were applied to the injury surface via a collagen sheet (Fig. 2A). Intense fluorescent signals from PKH 26-labeled EVs were detected at the

injury site along tendon fibers in ScxGFP tendon reporter mice 7 days after implantation (Fig. 2B). Most of EV positive signals were co-localized with DAPI positive and ScxGFP negative cells (arrow heads in Fig. 2C), indicating ASC EVs primarily target infiltrating inflammatory cells at the injury center.

Primed ASC EVs attenuate NF- κ B activity at the site of tendon injury and repair

The effects of EVs and iEV on the repair site inflammatory response were assessed in the NGL NF- κ B-luciferase reporter mice via live bioluminescence imaging (Fig. 3A).³¹ Results showed dramatic increases in NF- κ B activity at the repair site of untreated tendons at 3 days (Fig. 3, $P < 0.001$ vs. Pre) and 7 days (Fig. 3, $P = 0.042$ vs. Pre) but not at 1 day (Fig. 3, $P = 0.460$ vs. Pre) following repair. By contrast, iEV treatment led to an early and modest increase in NF- κ B activity at 1 day after repair (Fig. 3, $P = 0.021$ vs. Pre). This increase was retained at 3 days after repair (Fig. 3; $P = 0.034$ and 0.317 vs. pre and day 1, respectively) and substantially reduced at 7 days after repair (Fig. 3; $P = 0.548$, 0.011 , and 0.021 vs. Pre, D1, and D3, respectively). Overall, there were significant reductions of NF- κ B activity in iEV-treated tendons compared to untreated tendons at 3 days (Fig. 3, $P = 0.014$) and 7 days (Fig. 3, $P = 0.006$) after repair. EV treatment did not alter the NF- κ B activity in repaired tendons compared to the control repair (Fig. 3; $P = 0.521$, 0.193 and 0.364 vs. D1, D3 and D7, respectively). The NF- κ B activity in EV-treated tendons was over 2-fold that of iEV-treated tendons at 7 days after repair (Fig. 3, $P = 0.028$ vs. +iEV).

Primed ASC EVs reduce inflammatory gene expression in repaired tendons

The effect of ASC EVs on the tendon inflammatory response was further assessed at the gene expression level in Achilles tendons 7 days after repair by quantitative RT-PCR. In accordance with NF- κ B activation, the expression levels of examined inflammatory genes *Ifng*, *Nos2*, *Tnf*, and *Il6* were all significantly increased after tendon injury and repair (Fig. 4A–4D; $P = 0.000$, 0.001 , 0.000 , and 0.005 vs. paired intact tendons, respectively). Moreover, *Il1b*, which was barely detectable in intact tendons, became the most abundant inflammatory gene examined after tendon repair (Fig. 4E). Treatment with iEV but not EVs significantly reduced *Il1b* expression in repaired tendons (Fig. 4E, $P = 0.007$ vs. Repair and 0.011 vs. +EV). Similarly, significant differences in *Ifng* expression were detected among the three repair groups (Fig. 4A; \wedge , $P = 0.045$, one-way ANOVA) and iEVs but not EVs trended toward reducing *Ifng* expression after injury.

ASC iEVs facilitate tendon matrix gene expression after tendon injury

The expression levels of tendon matrix-related genes were also compared among the three repair groups 7 days after injury. While *Coll1a1* and *Col3a1* expression were increased in tendons from all three groups (Fig. 5A), *Mmp1*, a primary collagenase, which was undetectable in intact tendons, was induced after injury (Fig. 5A). Notably, treatment with both iEVs and EVs significantly attenuated the *Mmp1* expression (Fig. 5A; \wedge , $P = 0.007$, one-way ANOVA; $P = 0.013$ and 0.015 , +EV and +iEV vs. Repair, respectively) and iEV but not EV treatment further trended toward increasing both *Coll1a1* and *Col3a1* expression (Fig. 5A; $P = 0.057$ and 0.092 for *Coll1a1* and *Col3a1*, respectively, by one-way ANOVA). The tenogenic genes *Scx* and *Tnmd* were also increased in tendons from all groups; whereas, no significant group differences were detected (Fig. 5B). Unexpectedly, the cartilage matrix

gene *Col2a1* was increased in iEV-treated tendons (Fig. 5C; P=0.002 and 0.013 vs. Repair and +EV, respectively); and iEVs and EVs also increased *Sox9* expression (Fig. 5C; P=0.005 and 0.009, +iEV and +EV vs. Repair, respectively). Nevertheless, the resulting *Col2a1* level in iEV-treated tendons ($2^{-\text{Ct}}$: 3.47 ± 1.01) was less than 1% of the *Col1a1* level ($2^{-\text{Ct}}$: 398.34 ± 92.12). Moreover, tendon injury triggers substantial increases in the cartilage-degrading genes *Mmp13* and *Mmp3* expression in tendons from all three groups (Fig. 5C).

ASC iEVs reduce post-operative complications and facilitate anabolic tissue response after tendon injury

At the tissue level, iEV-treated tendons showed a much lower gap-rupture rate compared with untreated tendons (Fig. 6A; P=0.033 vs. Repair). Pentachrome staining on Achilles tendon sections revealed collagen in intact tendon in a bright red-orange color (Fig. 6C). The tendon is surrounded by a loose and fatty paratenon tissue (Fig. 6C, below a yellow dotted line). Tendon injury induced inflammatory cell infiltration and matrix deposition at the site of tendon injury (between the two dotted lines in Fig. 6D–6F) and within the adjacent paratenon (Fig. 6D–6F, below the yellow dotted lines). While we did not detect consistent histological differences in the cellularity and vascularity among tendons from the different repair groups, the iEV-treated tendons exhibited more collagen staining at the site of tendon injury than did untreated and EV-treated tendons (Fig. 6B, P<0.001 and P=0.004 vs. Repair and +EV, respectively; Fig. 6D–6F).

ASC iEVs are more effective than EVs in suppressing NF- κ B activation in macrophages

Next, we asked if the above observed *in vivo* effects of ASC EVs resulted from their ability to modulate the macrophage inflammatory response. NGL macrophages were co-cultured with either EVs or iEVs pre-labeled with PKH26 for 24h. Live fluorescence imaging detected PKH26 signals in nearly all cells without apparent differences between EVs (Fig. 7A) and iEVs (Fig. 7B). Moreover, a comparison between NGL (Fig. 7A and 7B) and wild type FVB macrophages (Fig. 7C) showed that macrophages with and without the NGL transgene took EVs with similar efficacy and that the EVs taken by either NGL or FVB macrophages were commonly localized to the cell bodies and not the protrusions.

The effects of EVs and iEVs on IL-1 β -induced NF- κ B activity in NGL macrophage were determined via a luciferin/luciferase-based assay. As shown in Fig. 7D, both EVs and iEVs but not CM or iCM blocked the IL-1 β -induced NF- κ B activity in macrophages (Fig. 7D; P=0.114, 0.276, 0.006 and 0.005, +CM, +iCM, +EV, and +iEV vs. Medium, respectively). Unexpectedly, while EVs were less effective than iEVs *in vivo*, the two treatments were equally effective *in vitro*. This difference may be due to a more extreme inflammatory environment present *in vivo*, which requires a more potent anti-inflammatory agent. To test this concept, we increased the concentration of IL-1 β from 5 ng/ml to 10 ng/ml and further compared the effect between EVs and iEVs on the NF- κ B-responsive luciferase transgene expression by the more sensitive quantitative real-time PCR. The result confirmed that, while both EV and iEV were effective in reducing IL-1 β -induced NF- κ B activity in macrophages (Fig. 7E; P=0.008 and P<0.0001, +EV and +iEV vs. Medium, respectively), iEVs were nearly three times more effective than EVs (P=0.004, +iEV vs. +EV).

DISCUSSION

Prior studies in our laboratory have shown that ASCs can shift the macrophage phenotypic response to tendon injury from a default pro-inflammatory M1 phenotype to a pro-regenerative M2 phenotype.^{10,11,17} Consistently, the findings of this study revealed that EVs, secreted by inflammation-stimulated ASCs, can attenuate the tendon inflammatory response in the earliest stages of healing after acute tendon injury and repair. Specifically, ASC EVs attenuated NF- κ B activity at the injury site and reduced pro-inflammatory cytokine *Il1b* and the major collagenase *Mmp1* expression. The effects of ASC EVs were coupled with their ability to directly target macrophages and to inhibit macrophage NF- κ B signaling. ASCs have been found to facilitate regenerative healing by promoting collagen synthesis within the repair site.¹¹ Similarly, ASC EVs were found to facilitate collagen gene expression and matrix production in injured tendons and to reduce post-operative rupture/gap formation. Moreover, a side-by-side comparison between ASC-produced EVs and soluble factors demonstrated that the anti-inflammatory paracrine function of ASCs is primarily mediated by EVs. Collectively, our results support the concept that ASC EVs are a promising substitute for ASCs as a therapeutic agent for tendon injury.

While the detailed mechanisms by which ASC EVs facilitate early tendon healing remain to be determined, our results support the concept that the effect is at least partially due to the ability of ASC EVs to attenuate the macrophage inflammatory response. Specifically, this study revealed that ASC EVs primarily target infiltrating inflammatory cells at the site of tendon injury and subsequently reduce NF- κ B activity and downstream *Il1b* expression in injured tendons. Our *in vitro* results further demonstrated that EVs can directly target macrophages and can block the inflammatory NF- κ B signaling in these cells. Consistent with these findings, a recent study showed that MSC-derived EVs can drive macrophage differentiation toward the anti-inflammatory M2 phenotype and that implantation of EV-educated M2 macrophages can promote early tendon healing.²⁷ In addition to macrophages, this study found that some ASC EVs were co-localized with tenocytes near the injury center. Therefore, ASC EVs may also directly facilitate tendon cell activity and function during tendon healing.

Our findings revealed that EVs produced by IFN γ -primed ASCs are more effective than EVs produced by naïve ASCs in curbing the inflammatory response in isolated macrophages and in repaired tendons. These findings are supported by several independent reports indicating that inflammation-stimulated stem cell EVs possess enhanced immunosuppressive functions^{21,26}, and improved therapeutic efficacy in treating inflammation-related conditions.^{24,37} The priming effect has been reported to be associated with selective enrichment of certain regulatory microRNA cargos in primed EVs, such as let-7b and miR-146a, which are capable of modulating the macrophage inflammatory response.^{24,37} It remains to be determined if a similar mechanism contributes to the iEV effects discovered in this study. Additionally, priming may modify the cell and tissue selectivity and therefore the effects of EVs. While this study found that macrophages take EVs and iEVs with similar efficacy in culture, a future study will be necessary to assess the possibility *in vivo*. The observed functional plasticity of ASCs and the potential dynamics of EV cargos introduce

an opportunity to harness EV functions by controlling the biochemical environments of ASCs and, more directly, by controlling the active components of EV cargos.

This study detected significant increases in the cartilage-related genes *Col2a1* (16-fold) and *Sox9* (4-fold) expression in iEV-treated tendons. While cartilage matrix formation is undesirable in normal tendon tissue, the increases noted after tendon injury and repair might be protective. This concept is supported by our observations that tendon injury triggered substantial increases in *Mmp13* (764-fold) and *Mmp3* (37-fold) expression and both MMP3 and MMP13 preferentially degrade type II collagen and proteoglycan.^{38,39} Type II collagen and proteoglycan are constituents of tendon extracellular matrices. Therefore, the *Sox9* and *Col2a1* increases caused by iEV that counteract the *Mmp13* and *Mmp3* increases after tendon injury may be beneficial for tendon healing. Consistently, at the tissue level, the iEV-treated tendons showed a substantially lower rupture/gap formation rate than did untreated tendons. Moreover, the pentachrome staining that illustrated proteoglycan and cartilage in a green-blue color at the calcaneus and Achilles tendon enthesis did not detect cartilage formation but did demonstrate a higher percentage of collagen at the midsubstance of all three iEV-treated tendons examined. The role of cartilage matrix formation during tendon repair will be investigated in a future study.

There are several potential limitations of this study. First, as this study focused on the impact of ASC EVs in the early stage of tendon healing, only one time point was investigated. It remains to be determined if the favorable effects of ASC EVs in this early stage of healing will lead to improved functional outcomes in the long term. Second, gene expression analysis in repaired tendons is not cell-type specific; only a selective group of genes was assessed; and changes in gene expression do not necessarily lead to changes in protein expression. Therefore, our results may not reveal the full spectrum of ASC EV function in tendon healing. Future RNA-sequencing and proteomics studies in isolated macrophages and tenocytes following ASC EV treatment will be helpful in addressing this issue. Third, the dose of IFN γ used to produce iEVs is based on a previous study focusing on the immunoregulatory function of ASCs.¹⁷ A dose-response relationship between IFN γ and the effect of iEVs on the macrophage inflammatory response needs to be further determined. Moreover, the active EV cargos and the underlying molecular mechanisms that contribute to the observed effects are yet to be identified.

In summary, this is the first *in vivo* study of ASC-derived extracellular vesicles in tendon healing. Our results establish the concept that ASC EVs, similar to ASCs, can attenuate the repair site inflammatory response and can facilitate tendon matrix regeneration in the earliest stage of tendon healing. These findings introduce a new opportunity for the biological treatment of tendon injury.

ACKNOWLEDGEMENTS

HS is an inventor with a pending patent that covers the ASC EVs and collagen sheet used in this study. This study is partially supported by the NIH R01 AR062947 and the Foundation for Barnes-Jewish Hospital. We thank the Washington University Musculoskeletal Research Center (NIH P30 AR057235), Molecular Imaging Center (NIH P50 CA094056), and Wandy Beatty for their respective histology, bioluminescence imaging, and transmission electron microscopy services. We thank Dr. Stavros Thomopoulos for his helpful feedback during the development

of the project and preparation of the manuscript and Dr. Phyllis Hanson for her input on EV biology and technologies.

REFERENCES

1. Butler DL, Juncosa N, Dressler MR. 2004 Functional efficacy of tendon repair processes. *Annu Rev Biomed Eng* 6: 303–329. [PubMed: 15255772]
2. Pennisi E Tending tender tendons. 2002. *Science* 295: 1011. [PubMed: 11834816]
3. Linderman SW, Gelberman RH, Thomopoulos S, Shen H Cell and biologic-based treatment of flexor tendon injuries. 2016. *Oper Tech Orthop* 26: 206–215. [PubMed: 28042226]
4. Manning CN, Havlioglu N, Knutsen E, et al. 2014 The early inflammatory response after flexor tendon healing: a gene expression and histological analysis. *J Orthop Res* 32: 645–652. [PubMed: 24464937]
5. Gelberman RH, Shen H, Korpakakis I, et al. 2016 Effect of adipose-derived stromal cells and BMP12 on intrasynovial tendon repair: A biomechanical, biochemical, and proteomics study. *J Orthop Res* 34: 630–640. [PubMed: 26445383]
6. Thomopoulos S, Parks WC, Rifkin DB, Derwin KA. 2015 Mechanisms of tendon injury and repair. *J Orthop Res* 33: 832–839. [PubMed: 25641114]
7. Schneider M, Angele P, Järvinen TAH, Docheva D. 2018 Rescue plan for Achilles: Therapeutics steering the fate and functions of stem cells in tendon wound healing. *Adv Drug Deliv Rev* 129: 352–375. [PubMed: 29278683]
8. Leong DJ, Sun HB. 2016 Mesenchymal stem cells in tendon repair and regeneration: basic understanding and translational challenges. *Ann N Y Acad Sci* 1383: 88–96. [PubMed: 27706825]
9. Aktas E, Chamberlain CS, Saether EE, et al. 2017 Immune modulation with primed mesenchymal stem cells delivered via biodegradable scaffold to repair an Achilles tendon segmental defect. *J Orthop Res* 35: 269–280. [PubMed: 27061844]
10. Shen H, Korpakakis I, Havlioglu N, et al. 2016 The effect of mesenchymal stromal cell sheets on the inflammatory stage of flexor tendon healing. *Stem Cell Res Ther* 7: 144. [PubMed: 27677963]
11. Gelberman RH, Linderman SW, Jayaram R, et al. 2017 Combined administration of ASCs and BMP-12 promotes an M2 macrophage phenotype and enhances tendon healing. *Clin Orthop Relat Res* 475: 2318–2331. [PubMed: 28462460]
12. Lipner J, Shen H, Cavinatto L, et al. 2015 In vivo evaluation of adipose-derived stromal cells delivered with a nanofiber scaffold for tendon-to-bone repair. *Tissue Eng Part A* 21: 2766–2774. [PubMed: 26414599]
13. Phinney DG, Prockop DJ. 2007 Concise review: mesenchymal stem/multipotent stromal cells: the state of transdifferentiation and modes of tissue repair—current views. *Stem Cells* 25: 2896–2902. [PubMed: 17901396]
14. Gimble JM, Grayson W, Guilak F, et al. 2011 Adipose tissue as a stem cell source for musculoskeletal regeneration. *Front Biosci (Schol Ed)* 3: 69–81. [PubMed: 21196358]
15. Kapur SK, Katz AJ. 2013 Review of the adipose derived stem cell secretome. *Biochimie* 95: 2222–2228. [PubMed: 23770442]
16. Hofer HR, Tuan RS. 2016 Secreted trophic factors of mesenchymal stem cells support neurovascular and musculoskeletal therapies. *Stem Cell Res Ther* 7: 131. [PubMed: 27612948]
17. Manning CN, Martel C, Sakiyama-Elbert SE, et al. 2015 Adipose-derived mesenchymal stromal cells modulate tendon fibroblast responses to macrophage-induced inflammation in vitro. *Stem Cell Res Ther* 6: 74. [PubMed: 25889287]
18. Zhang B, Yin Y, Lai RC, et al. 2014 Mesenchymal stem cells secrete immunologically active exosomes. *Stem Cells Dev* 23: 1233–1244. [PubMed: 24367916]
19. Lo Sicco C, Reverberi D, Balbi C, et al. 2017 Mesenchymal Stem Cell-Derived Extracellular Vesicles as Mediators of Anti-Inflammatory Effects: Endorsement of Macrophage Polarization. *Stem Cells Transl Med* 6: 1018–1028. [PubMed: 28186708]
20. Robbins PD, Morelli AE. 2014 Regulation of Immune Responses by Extracellular Vesicles. *Nat Rev Immunol* 14: 195–208. [PubMed: 24566916]

21. Domenis R, Cifù A, Quaglia S, et al. 2018 Pro inflammatory stimuli enhance the immunosuppressive functions of adipose mesenchymal stem cells-derived exosomes. *Sci Rep* 8: 13325. [PubMed: 30190615]
22. Yáñez-Mó M, Siljander PR, Andreu Z, et al. 2015 Biological properties of extracellular vesicles and their physiological functions. *J Extracell Vesicles* 4: 27066. [PubMed: 25979354]
23. Valadi H, Ekström K, Bossios A, et al. 2007 Exosome-mediated transfer of mRNAs and microRNAs is a novel mechanism of genetic exchange between cells. *Nat Cell Biol* 9: 654–659. [PubMed: 17486113]
24. Ti D, Hao H, Tong C, et al. 2015 LPS-preconditioned mesenchymal stromal cells modify macrophage polarization for resolution of chronic inflammation via exosome-shuttled let-7b. *J Transl Med* 13: 308. [PubMed: 26386558]
25. Anderson JD, Johansson HJ, Graham CS, et al. 2016 Comprehensive Proteomic Analysis of Mesenchymal Stem Cell Exosomes Reveals Modulation of Angiogenesis via Nuclear Factor- κ B Signaling. *Stem Cells* 34: 601–613. [PubMed: 26782178]
26. Harting MT, Srivastava AK, Zhaorigetu S, et al. 2018 Inflammation-Stimulated Mesenchymal Stromal Cell-Derived Extracellular Vesicles Attenuate Inflammation. *Stem Cells* 36: 79–90. [PubMed: 29076623]
27. Chamberlain CS, Clements AB, Kink JA, et al. 2019 Extracellular vesicle-educated macrophages promote early Achilles tendon healing. *Stem Cells* 37: 652–662. [PubMed: 30720911]
28. Shen H, Gelberman RH, Silva MJ, et al. 2013 BMP12 induces tenogenic differentiation of adipose-derived stromal cells. *PLoS One* 8: e77613.
29. Shen H, Jayaram R, Yoneda S, et al. 2018 The effect of adipose-derived stem cell sheets and CTGF on early flexor tendon healing in a canine model. *Sci Rep* 8: 11078. [PubMed: 30038250]
30. Volarevic V, Markovic BS, Gazdic M, et al. 2018 Ethical and Safety Issues of Stem Cell-Based Therapy *Int J Med Sci* 15: 36–45. [PubMed: 29333086]
31. Everhart MB, Han W, Sherrill TP, et al. 2006 Duration and intensity of NF- κ B activity determine the severity of endotoxin-induced acute lung injury. *J Immunol* 176: 4995–5005. [PubMed: 16585596]
32. Pryce BA; Brent AE; Murchison ND, et al. 2007 Generation of transgenic tendon reporters, ScxGFP and ScxAP, using regulatory elements of the scleraxis gene. *Dev Dyn* 236: 1677–1682. [PubMed: 17497702]
33. Dominici M, Le Blanc K, Mueller I, et al. 2006 Minimal criteria for defining multipotent mesenchymal stromal cells. The International Society for Cellular Therapy position statement. *Cytotherapy* 8:315–317. [PubMed: 16923606]
34. Yoneda S, Okubo H, Linderman SW, et al. 2018 The effect of modified locking methods and suture materials on Zone II flexor tendon repair-An ex vivo study. *PLoS One* 13: e0205121.
35. Narayanan R, Huang CC, Ravindran S. 2016 Hijacking the Cellular Mail: Exosome Mediated Differentiation of Mesenchymal Stem Cells. *Stem Cells Int* 2016:3808674.
36. Campbell I 2007 Chi-squared and Fisher-Irwin tests of two-by-two tables with small sample recommendations. *Stat Med* 26: 3661–3675. [PubMed: 17315184]
37. Song Y, Dou H, Li X, et al. 2017 Exosomal miR-146a contributes to the enhanced therapeutic efficacy of interleukin-1 β -primed mesenchymal stem cells against sepsis. *Stem Cells* 35: 1208–1221. [PubMed: 28090688]
38. Klein T, Bischoff R. 2011 Physiology and pathophysiology of matrix metalloproteases. *Amino Acids* 4: 271–290.
39. Fosang AJ, Last K, Knäuper V, et al. 1996 Degradation of cartilage aggrecan by collagenase-3 (MMP-13). *FEBS Lett* 80: 17–20.

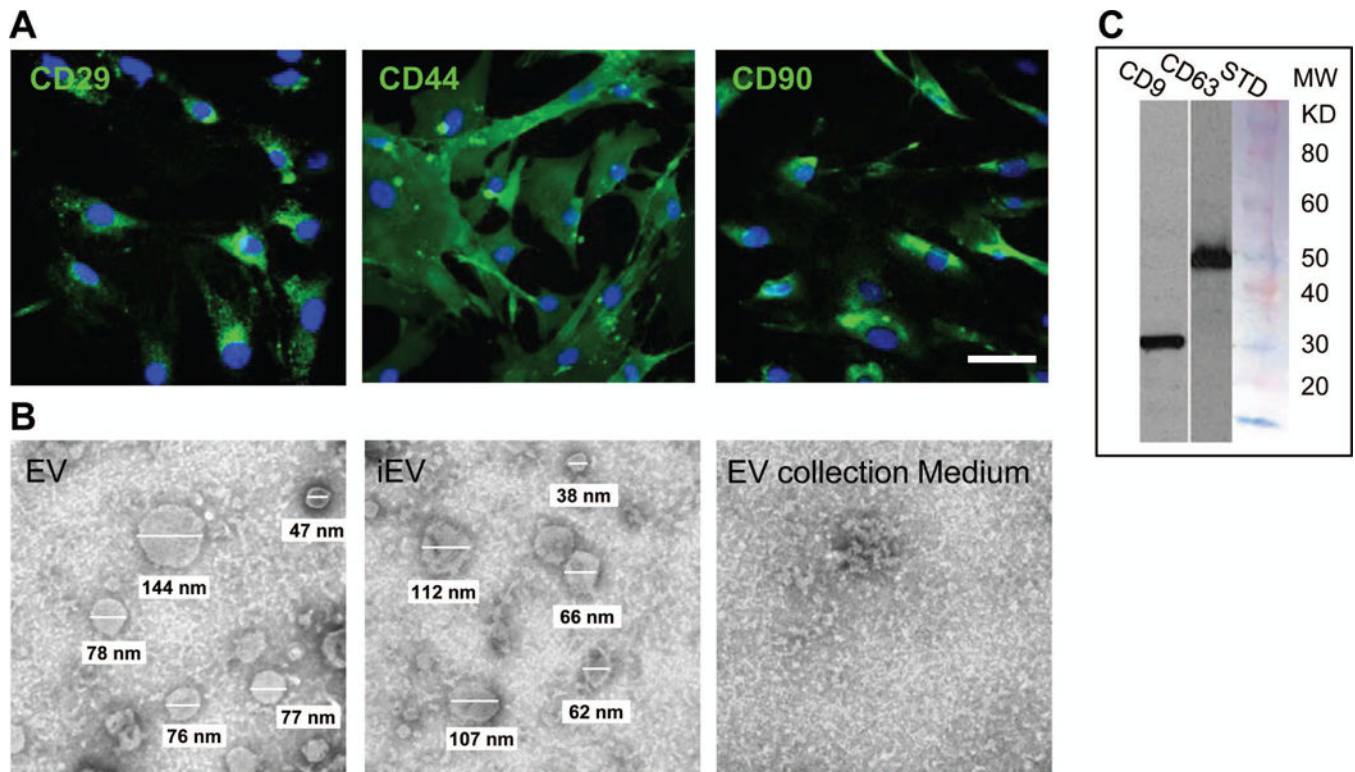


Figure 1.

Characterization of mouse ASCs and ASC EVs. **(A)** Representative immunofluorescence images of mouse ASCs stained with antibodies specific for the mesenchymal stem cell markers CD29, CD44, and CD90, respectively. Scale bar, 50 μ m. **(B)** Representative transmission electron microscopy images of mouse ASC EVs released by naïve (EV) and IFN γ -primed ASCs (iEV) along with the EV-free EV collection medium. **(C)** Western blot detects exosome markers CD9 and CD63 in isolated ASC EVs. STD, size standard. MW, molecular weight.

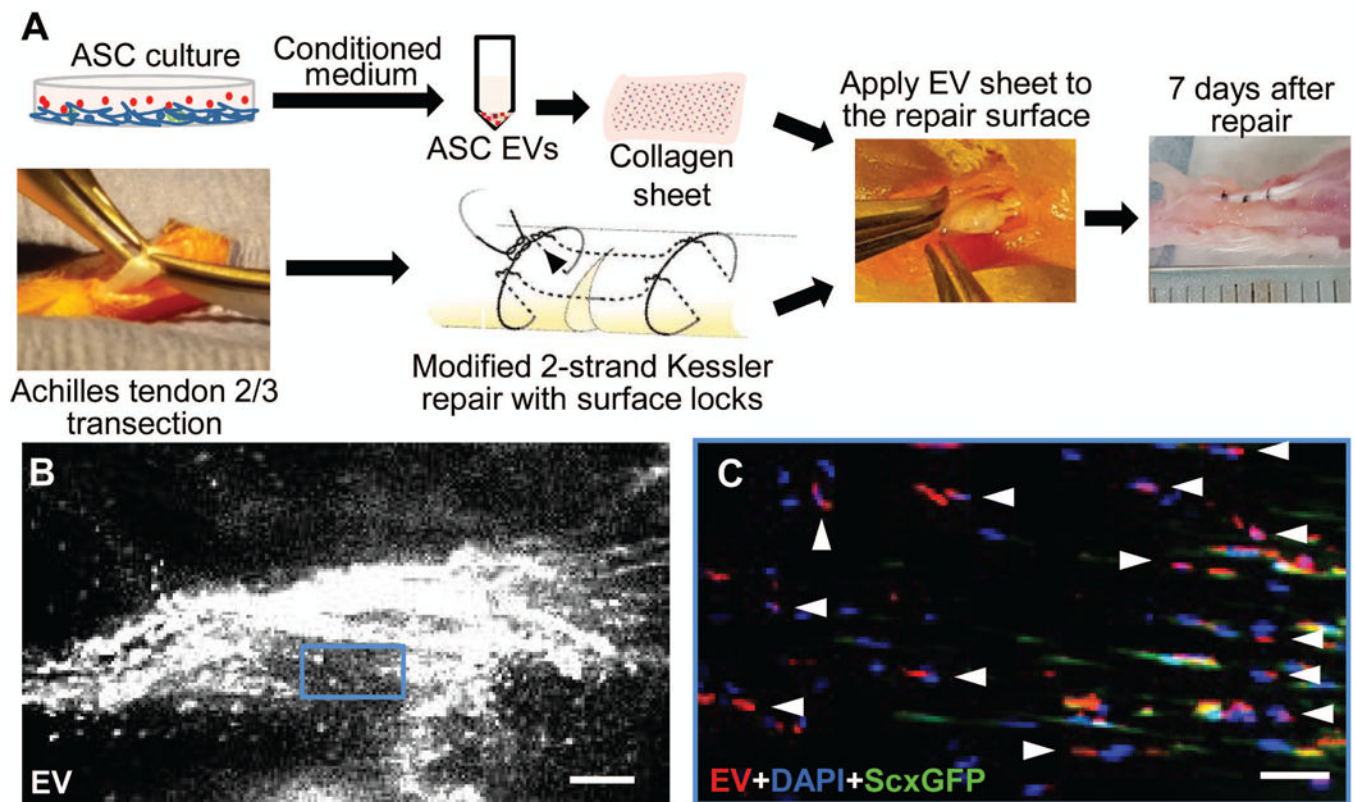


Figure 2. Application and localization of ASC EVs in a mouse model of Achilles tendon injury and repair. **(A)** A schematic illustration of the process of preparation and *in vivo* application of ASC EVs in a mouse model of Achilles tendon partial transection and repair. **(B)** A representative whole-mount fluorescence image showing the injury site of a mouse Achilles tendon 7 days after partial transection and application of ASC EVs. Scale bar, 100 μm . **(C)** A fluorescence image showing the sagittal section of the tendon shown in B at the boxed region. The residing tenocytes expressed ScxGFP. All cells were counterstained with DAPI. The arrow heads point to the EV positive signals at the DAPI positive and ScxGFP negative cells. Scale bar, 50 μm .

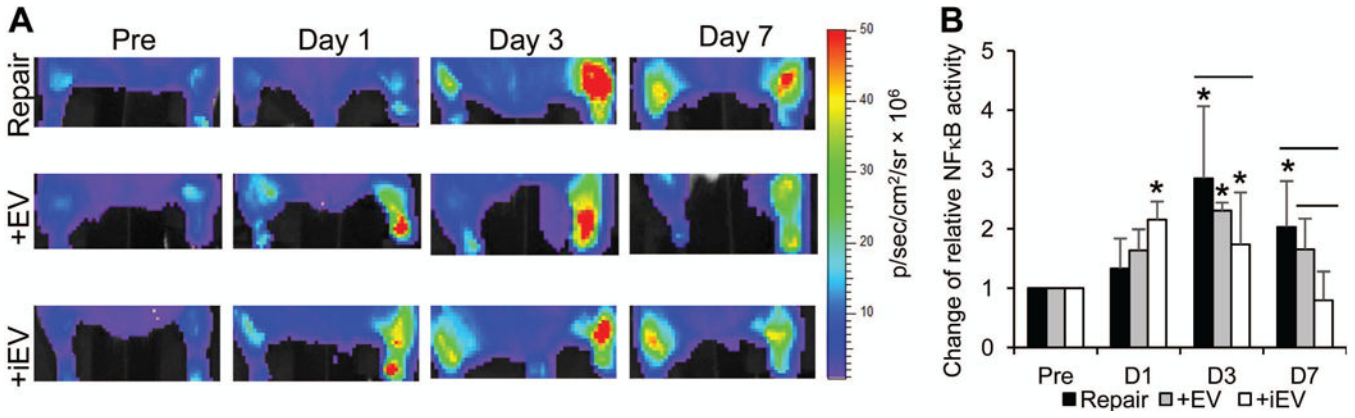


Figure 3. Representative bioluminescence images (A) and quantifications (B) of the changes in NF-κB activity at the repair site of NGL NF-κB reporter mice prior to (Pre) and at the indicated time points after right Achilles tendon repair and indicated treatments. * and —, P<0.05 by SNK multiple comparisons, compared to the pre-injury level of respective group and between indicated groups, respectively. No significant differences in NF-κB activity were detected among three repair groups prior to tendon injury and repair.

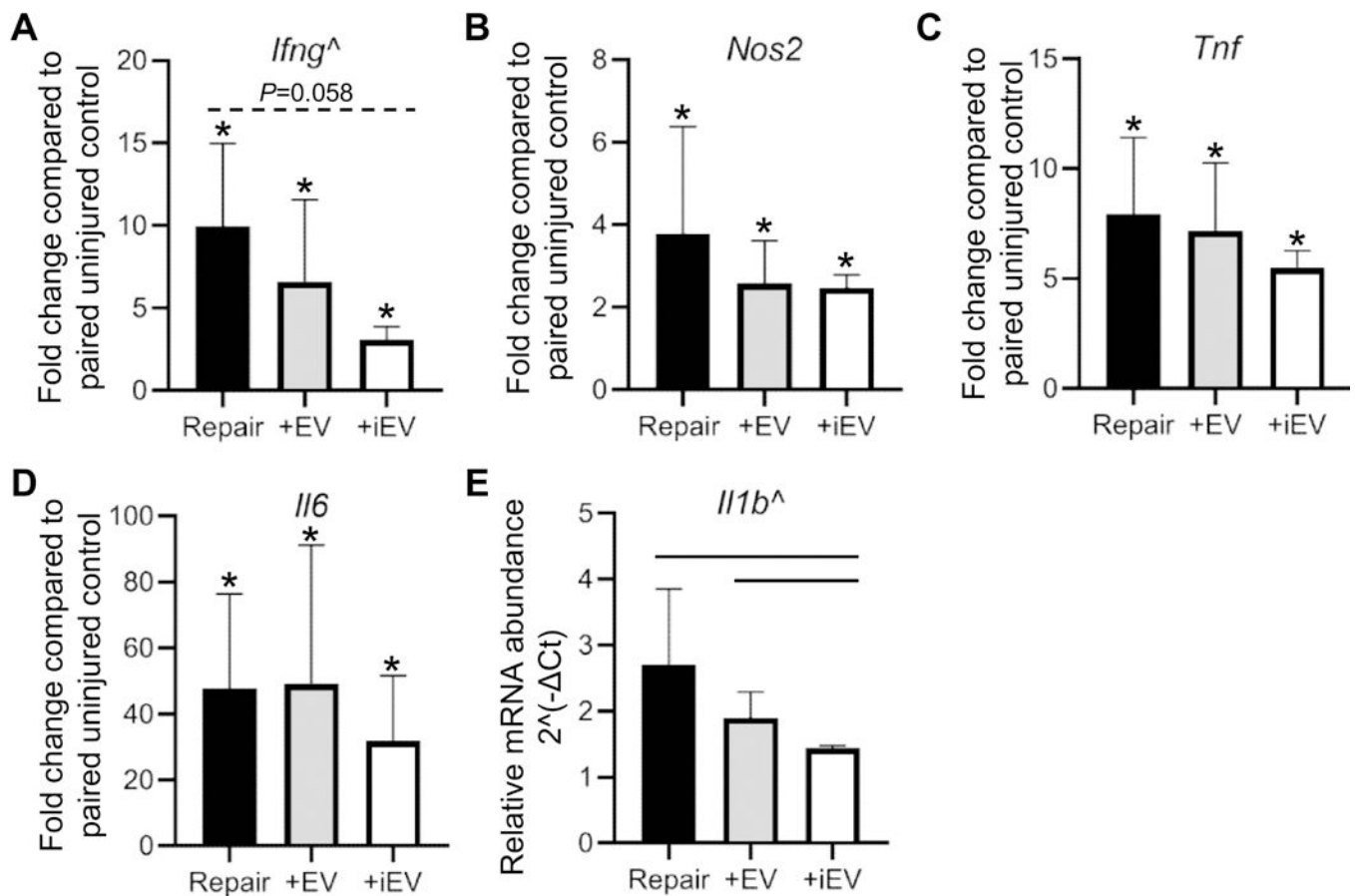


Figure 4.

Changes in the relative mRNA abundances of inflammatory genes in mouse Achilles tendons 7 days after tendon repair and indicated treatments. *, $P < 0.05$ compared to contralateral intact tendons by paired t-test; [^], $P < 0.05$ by one-way ANOVA. —, $P < 0.05$ between the indicated groups by Dunn's test.

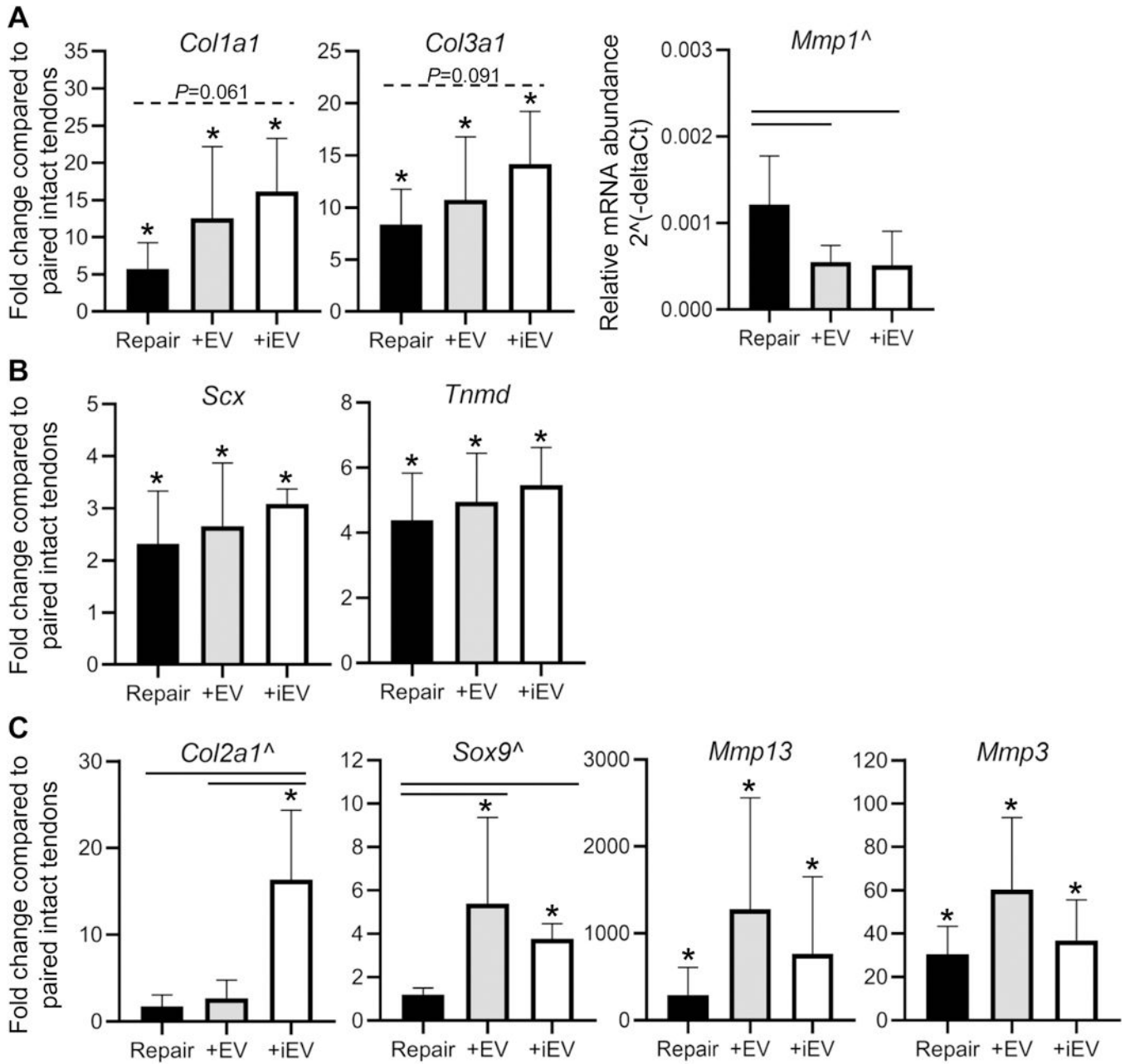


Figure 5. Changes in the relative mRNA abundances of tendon matrix-related genes in mouse Achilles tendons 7 days after tendon repair and indicated treatments. *, $P < 0.05$ compared to paired uninjured tendons by paired t-test; [^], $P < 0.05$ by one-way ANOVA. —, $P < 0.05$ between the indicated groups by Tukey's or Dunn's test (when appropriate).

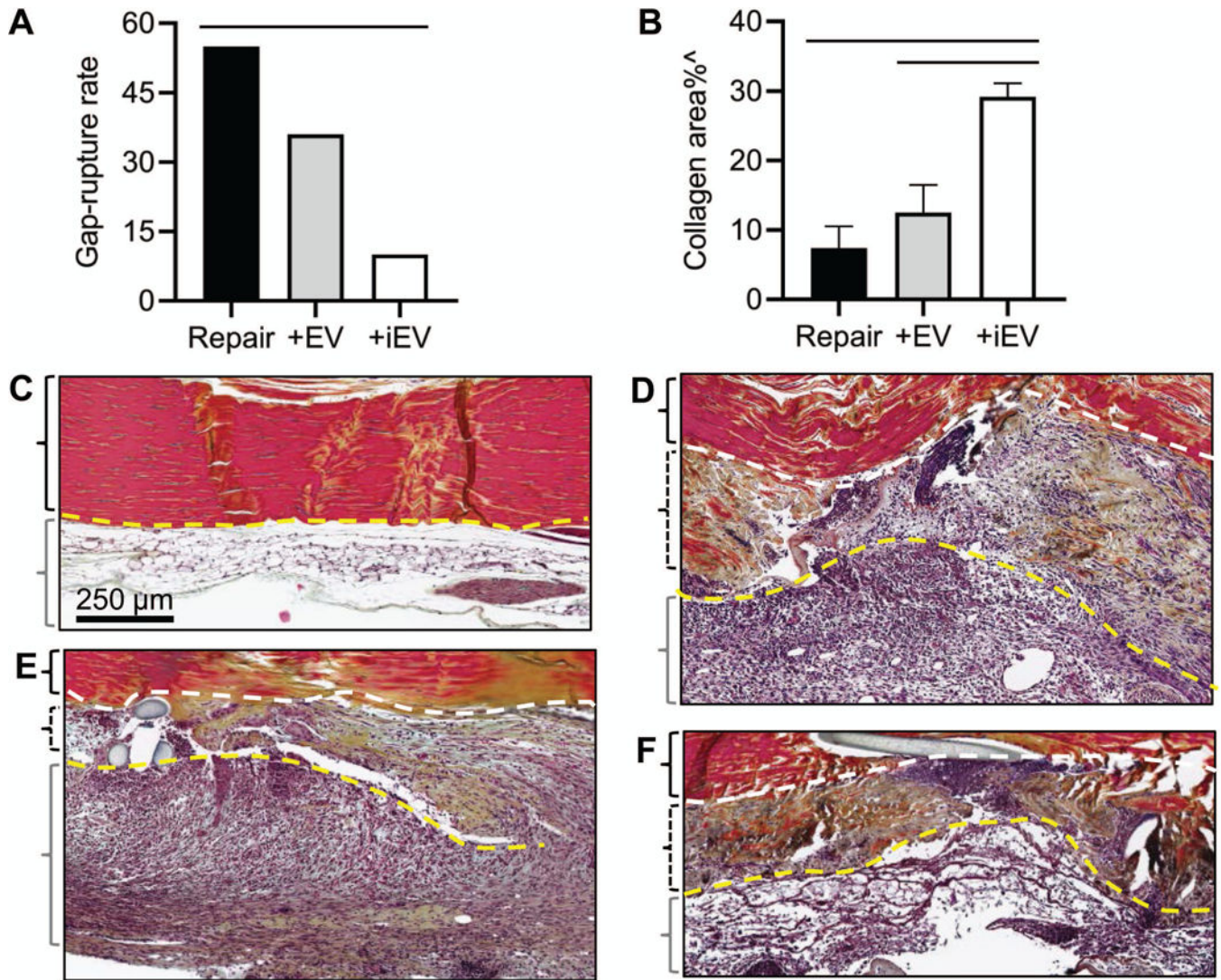


Figure 6.

Effects of ASC EVs on the tendon healing response 7 days after tendon injury and repair.

(A) A comparison of gap and rupture rates of injured Achilles tendons from Repair, +EV and +iEV groups. —, $P < 0.05$ between the indicated groups by an N-1 chi-squared test. (B) A comparison of the percentage of collagen-stained areas within the injured Achilles tendons from the indicated groups. [^], $P < 0.05$ by one-way ANOVA. —, $P < 0.05$ between the indicated groups by Tukey's test. (C-F) Representative images of pentachrome-stained coronal sections of Achilles tendons from an intact (C) and partial transected Achilles tendons from repair only (repair, D), EV-treated (+EV, E), and iEV-treated (+iEV, F) groups. Scale bar in C applied to C-F. The yellow dotted lines delineate the boundaries between Achilles tendons and the surrounding paratenon tissues. The white dotted lines delineate the boundaries between the intact and the transected portions of repaired Achilles tendons. The black braces enclose the intact (C) or the intact portions (D-F) of Achilles tendons; the dotted black braces enclose the transected portions of repaired Achilles tendons; and the grey braces enclose the paratenon region of Achilles tendons.

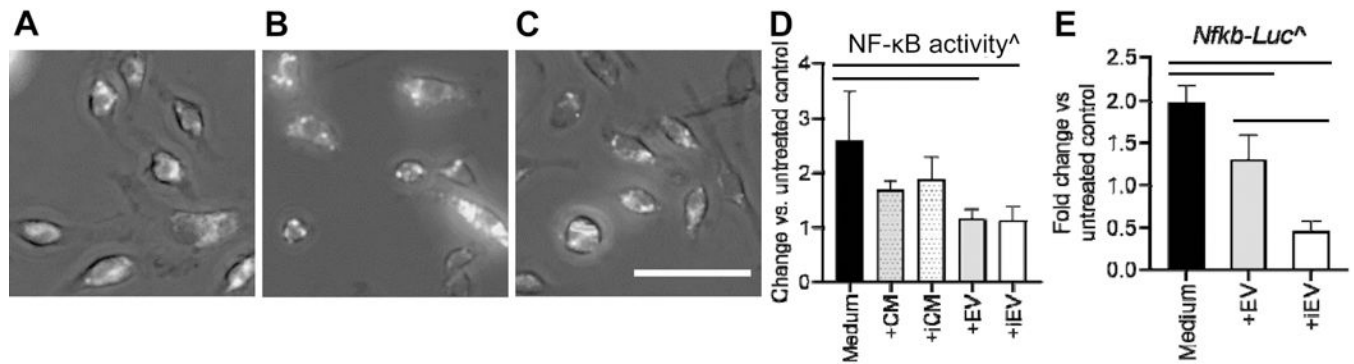


Figure 7.

Impacts of ASC EVs on the macrophage inflammatory response *in vitro*. (A-C)

Representative superimposed fluorescence and bright field images of isolated NGL (A, B) and FVB (C) macrophages co-cultured with fluorescently labeled EVs (A, C) or iEVs (B). Scale bar, 50 μ m. (D)

Changes in NF- κ B activity in macrophages pre-treated with control medium (Medium), EV-free conditioned medium from naïve ASCs (+CM), EV-free conditioned medium from primed ASCs (+iCM), EVs from naïve ASCs in control medium (+EV), or EVs from primed ASCs in control medium (+iEVs) 6 hours after IL-1 β treatment (5 ng/ml). (E) Changes in NF- κ B-responsive luciferase transgene (*Nfkb-Luc*) expression in isolated macrophages pre-treated with control medium (Medium), EVs (+EVs) or iEVs (+iEV) 24 hours after IL-1 β treatment (10 ng/ml). ^, P<0.05 by one-way ANOVA in D and E. —, P<0.05 between the indicated groups by Tukey's test in D and E.

^, P<0.05 by one-way ANOVA in D and E. —, P<0.05 between the indicated groups by Tukey's test in D and E.

Table 1.

Commercial primers used for real-time PCR

Gene symbol	Gene name	Assay number	Accession number	Amplicon (nt)
<i>Coll1a1</i>	collagen, type I, alpha 1	QT00162204	NM_007742	98
<i>Col2a1</i>	collagen, type II, alpha 1	QT01055523	NM_001113515	60
<i>Col3a1</i>	collagen, type III, alpha 1	QT2331301	NM_009930	73
<i>Il1b</i>	interleukin 1, beta	QT01048355	NM_008361	150
<i>Mmp3</i>	matrix metalloproteinase 3	QT00107751	NM_010809	146
<i>Mmp13</i>	matrix metalloproteinase 13	QT00111104	NM_008607	96
<i>Scx</i>	scleraxis	QT00166271	NM_198885	67
<i>Sox9</i>	SRY (sex determining region Y)-box 9	QT00163765	NM_011448	124
<i>Tnf</i>	tumor necrosis factor	QT00104006	NM_013693	112
<i>Tnmd</i>	tenomodulin	QT00126427	NM_022322	100

Table 2.

Custom primers used for real-time PCR.

Gene symbol	Accession #	Forward primer	Reverse primer	Amplicon (nt)
<i>Ifng</i>	NM_008337.4	atctggaggaactggcaaaa	ttcaagactcaaagagtctgagg	89
<i>Ipo8</i>	NM_001081113.1	cacattgctcgtctcttt	acctgttgaattcccactgc	112
<i>Il6</i>	NM_001314054.1	gctaccaactggatataatcagga	ccaggtagctatgggtactccagaa	77
<i>Mmp1a</i>	NM_032006	tgtgttcacaacggagacc	gccaagtgttagtagtttcca	73
<i>Nos2</i>	NM_010927.4	cttgccacggacgagac	tcattgtactctgaggctgac	66
<i>NF-kb_Luc</i>	AP018660.1	gcaggcagttctatgaggca	gaaatgccgttcggttggc	476

Author Manuscript

Author Manuscript

Author Manuscript

Author Manuscript